MRP4-Mediated Regulation of Intracellular cAMP and cGMP Levels in Trabecular Meshwork Cells and Homeostasis of Intraocular Pressure

Padmanabhan P. Pattabiraman,[1] *Paula E. Pecen,*[1] *and Ponugoti Vasantha Rao*[1,2]

Purpose. Multidrug, resistance-associated protein-4 (MRP4) is a membrane transporter that regulates the cellular efflux of cyclic nucleotides (cAMP and cGMP) involved in various physiologic responses. This study examined the expression and distribution of MRP4 in the trabecular meshwork (TM) cells and its role in homeostasis of IOP.

Methods. Expression and distribution of MRP4 in human TM (HTM) cells and aqueous humor (AH) outflow pathway was determined by RT-PCR, immunoblotting, and immunofluorescence. Effects of inhibiting MRP4 activity and suppression of MRP4 expression on cAMP and cGMP levels, myosin light chain (MLC) phosphorylation, actin filament organization and activity of protein kinase G (PKG), protein kinase A (PKA), Rho guanosine triphosphatase (GTPase), and MLC phosphatase was monitored in HTM cells using ELISA, siRNA, biochemical, and immunofluorescence analyses. Topical application of the MRP4 inhibitor MK571 was tested to assess changes in IOP in rabbits.

Results. RT-PCR, immunoblot, and immunofluorescence analyses confirmed the expression of MRP4 in HTM cells and distribution in human AH outflow pathway. Inhibition of MRP4 in HTM cells by MK571 or probenecid resulted in cell shape changes and decreases in actin stress fibers and MLC phosphorylation. Levels of intracellular cAMP and cGMP in HTM cells were increased significantly under these conditions. MK571-induced HTM cell relaxation appeared to be mediated predominantly via activation of the cGMP-dependent PKG signaling pathway. Topical application of MK571 significantly decreased IOP in Dutch-Belted rabbits.

Conclusions. These observations reveal that cyclic nucleotide efflux controlling transporter-MRP4 plays a significant role in IOP homeostasis potentially by regulating the relaxation characteristics of AH outflow pathway cells. (*Invest Ophthalmol Vis Sci.* 2013;54:1636–1649) DOI:10.1167/iovs.12-11107

Glaucoma is an optic neuropathy accounting for the second leading cause of blindness in the world. Global estimates indicate that over 60 million people currently suffer from glaucomatous neuropathy, which, if not treated adequately and in a timely manner, can result in irreversible blindness in many of these patients.[1] POAG, which is the most prevalent type of glaucoma, is commonly associated with elevated IOP caused by impaired drainage of aqueous humor (AH).[2,3] Importantly, elevated IOP is a primary risk factor for POAG.[2,3] IOP is determined by the balance between secretion of AH by the nonpigmented ciliary epithelium and its drainage from the eye anterior chamber via both the conventional and nonconventional routes.[2,3] The conventional outflow pathway consists of the trabecular meshwork (TM) and Schlemm's canal (SC) and accounts for over 80% of total AH drainage.[2–4] It is generally believed that impaired AH outflow through the conventional pathway is the main cause for elevated IOP in glaucoma patients,[2–4] however, the molecular and cellular basis for increased resistance to AH outflow remains to be clarified. Therefore, identifying and characterizing molecular mechanisms regulating AH outflow is important and necessary to support the development of novel and targeted therapies for treatment of elevated IOP in glaucoma patients.[4,5]

The contractile and relaxation characteristics, and adhesive interactions of TM cells with the extracellular matrix (ECM), together with the tissue material properties of TM, are considered to be attributes that influences AH outflow via the conventional pathway.[5–10] Support for this speculation derives from observations indicating that activation and inhibition of contractile activity of TM cells by actomyosin cytoskeletal integrity, myosin II phosphorylation, and ECM organization reciprocally influence AH outflow and IOP in various model systems.[5,7–10] Additionally, various intracellular signaling responses mediated by protein kinase C, Rho/Rho kinase, myosin light chain (MLC) kinase, extracellular signal-regulated kinase (ERK kinase), Wnt and calcium have also been demonstrated to modulate AH outflow and IOP.[7–18] Interestingly, the intracellular cyclic nucleotides cAMP and cGMP, which are known to regulate the relaxation characteristics of smooth muscle tissue including the TM via protein kinase (PK)A and PKG, have been reported to influence AH outflow and IOP.[19–28] However, different cellular mechanisms regulating the levels of intracellular cAMP and cGMP in cells of the AH outflow pathway and their involvement in the relaxation characteristics of TM tissue and cells are not completely understood. Adenylate and guanylate cyclases, which are activated by external cues such as nitric oxide and adenosine, generate and regulate the levels of intracellular cAMP and cGMP that in turn control different cellular processes including cellular relaxation via the PKA- and PKG-dependent signaling pathways.[21–23] Degradation of cyclic nucleotides is regulated by cyclic nucleotide phosphodiesterases.[21,23] TM cells and tissues of the AH outflow pathway have been demonstrated to express both the cyclases and phosphodiesterases and they have been reported to participate in modulation of AH outflow in different species.[20,24–30]

From the Departments of [1]Ophthalmology and [2]Pharmacology and Cancer Biology, Duke University School of Medicine, Durham, North Carolina.

Supported by an R01 grant from the National Institutes of Health (EY018590).

Submitted for publication October 9, 2012; revised January 7, 2013; accepted January 26, 2013.

Disclosure: **P.P. Pattabiraman**, None; **P.E. Pecen**, None; **P.V. Rao**, None

Corresponding author: Ponugoti Vasantha Rao, Department of Ophthalmology, Duke University School of Medicine, Durham, NC 27710; rao00011@mc.duke.edu.

Investigative Ophthalmology & Visual Science, March 2013, Vol. 54, No. 3

Table. Primer Sequences Used to Amplify MRP Subtypes in HTM Cells

Name	Primer Sequence, Forward/Reverse	Product Size, bps
hMRP1	CAT GAA GGC CAT CGG ACT CT/CAG GTC CAC GTG CAG ACA	258
hMRP2	GAC TAT GGG CTG ATA TCC AGT GT/AGG CAC TCC AGA AAT GTG CT	489
hMRP3	GGC ACT GCT GAT TGA AGA CA/AAT GGC TGC TTT CTC CTC CT	228
hMRP4	CCA TTG AAG ATC TTC CTG G/GGT GTT CAA TCT GTG TGC	197
hMRP5	GGA TAA CTT CTC AGT GGG/GGA ATG GCA ATG CTC TAA AG	381
hMRP6	TCA GAA GCC CAG ACA GAG GT/CCC AGC GTA GAG GAG AAA CA	596
hMRP8	TCT GCG ACC TTC TTG TTT GG/TCA GTA CAG CAT TTG CAA CAC TT	259

In addition to the direct control manifested via rates of synthesis and degradation, intracellular concentration of cAMP and cGMP can be also controlled at the level of cellular efflux regulated by specific membrane transporters.[31,32] The C subfamily of adenosine triphosphate (ATP)-binding cassette (ABCC) transporters is comprised of nine multidrug resistance-associated channel proteins (MRPs) involved in pumping various organic anionic compounds out of the cell.[32] Of the different ABCC transporters, MRP4, and MRP5 have been demonstrated to drive cellular efflux of various endogenous organic compounds including cAMP and cGMP, eicosanoids, and glutathione in an ATP-dependent manner, and to regulate diverse cellular responses.[31,33–36] MRP4 and MRP5 are expressed in various tissues and have been demonstrated to regulate smooth-muscle cell proliferation and relaxation.[31,37] Significantly, inhibition of MRP4 was recently shown to prevent and reverse pulmonary hypertension via regulating the relaxation characteristics of pulmonary arteries.[38]

Based on these physiologic attributes of the MRPs, we hypothesized that MRP4 might play a significant role in regulating TM cell relaxation characteristics and influence homeostasis of IOP. To evaluate this premise, we first profiled the expression and distribution of MRP4 in HTM cells and tissue prior to addressing the involvement of this transporter protein in TM cell relaxation properties and IOP homeostasis. We report that inhibition of MRP4 in HTM cells increases the levels of both cAMP and cGMP, results in cellular relaxation in TM cells via activation of cGMP-dependent PKG signaling, and leads to decreased IOP in live rabbits.

Materials and Methods

Reagents

MK571 sodium salt (3-[3-[2-(7-chloroquinolin-2-yl)vinyl]phenyl]-(2-dimethyl carbamoylethylsulfanyl) methylsulfanyl] propionic acid) (C.No. BML-RA109), cell permeable cGMP-dependent kinase inhibitor, an antagonist of cGMP: Rp-8-Br-cGMPS (C. No. BML-CN206), and cAMP-dependent kinase inhibitor, an antagonist of cAMP: Rp-8-Br-2′-O-MB-cAMPS (C. No. B010) were purchased from Enzo Life Sciences (Farmingdale, NY). quercetin (C. No. Q4951), probenecid (C. No. P8761), 3-Isobutyl-1-methylxanthine (IBMX; C. No. I5879), Phalloidin-tetramethylrhodamine B isothiocyanate (C. No. P1951), Phalloidin-Fluorescein isothiocyanate (C. No. P5282), and mouse monoclonal anti-β-Tubulin (C. No. T5293) were purchased from Sigma-Aldrich (St. Louis, MO). Rabbit anti-phospho-MLC (C. No. 3672), rabbit anti-total MLC (C. No. 3671), and rabbit anti-p vasodilation-stimulated phosphoprotein (VASP) Ser 157 (C. No. 3111), rabbit anti-pVASP Ser 239 (C. No. 3114), and rabbit anti-VASP (C. No. 3112) antibodies were procured from Cell Signaling Technology (Danvers, MA). Rabbit anti-phosphomyosin phosphatase targeting subunit 1 (MYPT1; C. No. ABS45) antibody was from Millipore (Danvers, MA). Rabbit anti-phospho-RhoA Ser-188 (C. NO. sc-32,954) antibody was from Santa Cruz Biotechnology (Santa Cruz, CA). Protease inhibitor cocktail tablets (complete Ultra tablets, Mini, EDTA-free) and phosphatase inhibitor cocktail tablets (PhosSTOP) were from Roche (Basel, Switzerland). The rabbit anti-human MRP4 antibody was a generous gift from Frans G.M. Russel, Professor of Pharmacology and Toxicology, University of Nijmegen, The Netherlands.

Cell Culture

Human primary TM cells were cultured from TM tissue isolated from freshly obtained corneal rings (from age groups of 42-, 58-, and 73-year-old donor eyes) after they had been used for corneal transplantation by the Duke Ophthalmology clinical service as we described earlier.[39] All experiments were conducted using confluent cultures passaged between four to six cycles (unless mentioned otherwise) and cells were maintained at 37°C under 5% CO_2, in Dulbecco's modified Eagle's medium (DMEM; GIBCO, Life Technologies, Grand Island, NY) containing 10% fetal bovine serum (FBS) and penicillin (100 U/500 mL)-streptomycin (100 μg/500 mL)-glutamine (4 mM). All cell culture experiments were performed with cells derived from minimum of two independent human donors after serum starvation for 24 hours.

Reverse Transcription-Polymerase Chain Reaction

Total RNA was extracted from confluent cultures (passage 3 or 4) of HTM cells (donors aged 33, 58, and 74 years) using RNeasy Micro kit (Qiagen, Valencia, CA) per manufacturer recommendations. Five micrograms of total RNA (free of DNA) were used for first-strand cDNA synthesis using the Superscript first-strand synthesis system (Life Technologies, Carlsbad, CA). The cDNA pools were subsequently screened for transcripts of various MRP subtypes using the respective forward and reverse primer sets (Table). Reactions lacking reverse transcriptase (negative RT) controls were carried out simultaneously. The PCR products were separated on a 1% agarose gel, visualized, and imaged using GelRed nucleic acid stain (RGB-4103) purchased from Phenix Research (Candler, NC) and a Fotodyne imaging system (Hartland, WI). The expected PCR size products (Table) were sequenced to confirm identity.

Immunohistochemistry

Tissue sections from formalin-fixed, paraffin-embedded human donor eye whole globes were immunostained as previously described.[39] Briefly, 5-μm thick tissue sections were deparaffinized and rehydrated using three changes of xylene, followed by three changes of absolute ethyl alcohol and washing with three changes of water. To unmask the antigen epitopes, heat-induced antigen retrieval was performed using 0.1 M citrate buffer pH 6.0 (Vector Laboratories, Burlingame, CA) for 20 minutes at 100°C. The slides were then blocked for nonspecific interaction with Biocare Medical's (Concord, CA) Sniper Background Reducer (C. No. BS966). The tissue sections were then incubated overnight at 4°C with rabbit polyclonal primary antibody raised against MRP-4 (dilution of 1:50) in a humidified chamber. Primary antibody dilutions were made in 1% bovine albumin in Tris-buffered saline (TBS). After incubation, the slides were washed three times with TBS and incubated with Alexa Fluor-594 goat anti-rabbit secondary antibodies (Life Technologies) for 2 hours at room temperature. Immunostaining analysis was carried out in triplicate, and a negative control (in the

presence of secondary antibody alone) was run simultaneously. After the final step of staining and washing, tissue sections were coverslipped using Aqua mount (Lerner Laboratories, Pittsburg, PA). The slides were then viewed and imaged using a Nikon C1 Digital Eclipse confocal system (Nikon Instruments, Melville, NY) with 20 and 60× objectives.

Actin Filament Staining

HTM cells were grown on gelatin (2%)–coated glass coverslips until they attained confluence. After appropriate treatments, cells were washed in PBS twice and then fixed, permeabilized, and stained for actin stress fibers using tertamethyl rhodamine isothiocyanate (TRITC)- or fluorescein isothiocyanate (FITC)-conjugated phalloidin as we described earlier.[9] The slides were viewed and imaged using a Nikon confocal system (C1 Digital Eclipse) with 40× objective.

Immunoblot Analysis

HTM cells were cultured to confluence on plastic petri plates. Total cell lysates, cytosolic and membrane-enriched fractions were prepared from serum-starved confluent cultures of control and drug-treated TM cells. For preparation of membrane-enriched protein fractions, cells were homogenized with hypotonic Tris buffer (10 mM Tris, 0.2 mM $MgCl_2$), pH 7.4, containing phosphatase and protease inhibitor cocktail and centrifuged for 15 minutes at 3000 rpm at 4°C. A portion of the supernatant was collected as the total protein fraction, with the rest of the supernatant being centrifuged at 40,000*g* for 1 hour at 4°C to generate the cytosolic fraction (supernatant) and a pellet, which was further processed as the membrane-enriched protein fraction. The pellet was washed and centrifuged twice at 40,000*g* for 1 hour at 4°C, then resuspended in a urea sample buffer containing 8 M urea and 0.5 M dithiothreitol (DTT). Bio-Rad protein assay reagent (C. No. 500-0006; Hercules, CA) was used to estimate protein concentration. Samples containing equal amounts of protein were mixed with Laemmli buffer and separated by SDS-PAGE (8% and 15% acrylamide), followed by transfer of resolved proteins to nitrocellulose membranes. Membranes were blocked for 2 hours at room temperature in TBS containing 0.1% Tween 20 and 5% (wt/vol) nonfat dry milk and subsequently probed with primary antibodies (anti-human MRP4, anti-pMYPT1, anti-pRhoA, anti-pVASP Ser 157, anti-pVASP Ser 239, or anti-total VASP) in conjunction with horseradish peroxidase-conjugated secondary antibodies.[9] Detection of immunoreactivity was performed by enhanced chemiluminescence (ECL). Densitometry of immunoblot films was performed using ImageJ software (National Institutes of Health, Bethesda, MD). Data were normalized to the specified loading controls.

Myosin Light Chain Phosphorylation

The effects of MK571, Probenecid, Quercetin, IBMX, PKA inhibitor Rp-8-Br-2′-O-MB-cAMPS, or PKG inhibitor Rp-8-Br-cGMPS on HTM cell MLC phosphorylation were determined by urea-glycerol gel electrophoresis and immunoblot analysis using anti-phospho-MLC antibody, as we described earlier.[9] Densitometry of immunoblot films was performed as described above and data were normalized to total MLC.

Measurement of Intracellular Cyclic Nucleotide Levels

cAMP and cGMP concentrations were measured using cyclic AMP XP assay kit (C. No. 4339) and cyclic GMP XP assay kit (C. No. 4360) (Cell Signaling Technology, Danvers, MA). This ELISA kit is based on competition between cAMP or cGMP found in the test sample and a fixed amount of horseradish peroxidase (HRP)-linked cAMP or cGMP for binding to anti-cAMP or anti-cGMP XP rabbit mAb immobilized onto a 96-well plate. Following washing to remove excess cAMP or cGMP and HRP-linked cAMP or cGMP, the HRP substrate 3, 3′, 5, 5′-tetramethyl benzidine (TMB) was added to develop color. Briefly, HTM cells were cultured in 6-well dishes at a density of 5×10^4. After overnight serum starvation, cells were treated with MK571 or IBMX for 30 minutes or IBMX for 15 minutes followed by MK571 for 30 minutes. The reactions were stopped by aspirating culture media and washing cells with cold PBS. Cells were then lysed with 100 μL of lysis buffer containing 20 mM Tris-HCL (pH 7.5), 150 mM NaCl, 1 mM EDTA, 1 mM EGTA, 1% Triton, 2.5 mM sodium pyrophosphate, 1 mM beta-glycerophosphate, 1 mM sodium orthovanadate, 1 μg/mL leupeptin, and 1 M phenylmethylsulfonyl fluoride (PMSF). 50 μL of cell lysate was transferred into microtiter plates and cAMP and cGMP concentrations were measured according to the protocol provided with the kit. In each experiment, a standard curve was generated in parallel and used to calculate cAMP and cGMP concentrations.

Small Interfering RNA Transfection

Small interfering RNA (siRNA) directed against the human MRP4 sequence (C. No. sc-40,750) and a corresponding, FITC-conjugated scrambled control siRNA (C. No. sc-36,869) were purchased from Santa Cruz Biotechnology. HTM cells were transfected using a 120 pM concentration of hMRP4 siRNA or control siRNA using an endothelial nucleofector Kit (Lonza, Basel, Switzerland), as per the manufacturer's instructions. hMRP4 siRNA was cotransfected with the green fluorescent protein (GFP) plasmid pmaxGFP provided in the kit. Following transfection, cells were plated either on glass coverslips or in plastic petri plates. Expression of GFP or appearance of FITC in the cells was followed to confirm transfection efficiency. Morphological changes were observed within 82 to 84 hours after transfection, after which the cells were fixed and immunostained or immunoblotted for proteins of interest.

IOP Measurements in Rabbits

Experiments were performed on four healthy Dutch-Belted male rabbits weighing around 5 pounds each, adhering to ARVO statement for the Use of Animals in Ophthalmic and Vision Research, per a protocol approved by the Duke Institutional Animal Care and Use Committee (IACUC). IOP was recorded using a pneumotonometer (Model 30; Medtronic Solan, Jacksonville, FL) after topical application of proparacaine (0.05%) as we described earlier.[40] One eye was treated with vehicle (PBS) and the other eye was treated with the drug (MK571) prepared in PBS. The drug was administered in two 30-μL drops with a 1 minute interval, and eyelids were kept open during drug application to prevent blinking. The baseline IOP was recorded just before drug application and at 1, 2, 4, 6, and 24 hours post drug application. Differences in IOP between the test and the control eyes at different time points and changes between baseline IOP and drug treated IOP were tested for statistical significance. Two different drug concentrations were tested (0.1% and 0.2% MK571) on four rabbits each, and the experiments were repeated twice on the same rabbits allowing sufficient interval between the tests.

Statistical Analyses

All data represent the average of results from a minimum of three to four independent experiments and values are presented as mean ± SD. Quantitative data were analyzed by Student's *t*-test (for biochemical changes) and Wilcoxon rank-sum test (for IOP). Minimum values of P less than 0.05 were considered as statistically significant.

Results

Expression and Distribution of MRP4 in Human TM Cells

PCR-based amplification of single stranded cDNA derived from three different batches of HTM cells (donor eyes of 33-, 58-, and 74-year-olds) for different isoforms of MRP genes,

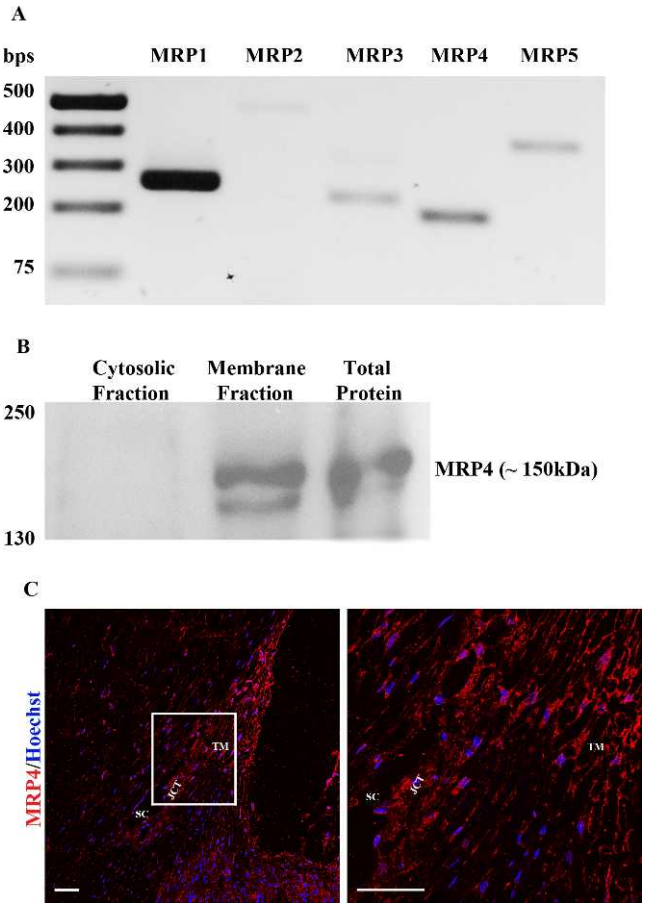

Figure 1. Expression and distribution of MRP4 in human TM cells and the AH outflow pathway. (**A**) RT-PCR analysis of HTM cell RNA confirmed the expression of MRP1, MRP2, MRP3, MRP4, and MRP5 genes. (**B**) Immunoblot analysis of MRP4 in the total, soluble, and membrane-rich fractions of human TM cells reveals a distinct immunopositive doublet protein band at approximately 150 kDa in the total and membrane-enriched fractions but not in the cytosolic fraction, confirming the expected membrane localization of MRP4. (**C**) Immunofluorescence-based analysis of the distribution profile of MRP4 in human AH outflow pathway tissues of the healthy eye indicates intense staining throughout the AH outflow pathway including TM, SC, and JCT. The panel on the right shows a magnified area (60× objective) of AH outflow pathway indicated by the rectangular box (20× objective) in the left panel. *Scale bar*: 50 μm.

produced detectable levels and expected size of amplified DNA specific for MRP1, MRP2, MRP3, MRP4, and MRP5 as shown in Figure 1A (results derived from a single TM cell strain are shown). Oligonucleotide primer sets specific for MRP6 and MRP8 (Table) did not yield detectable amounts of respective product under the conditions described in this study. Identity of individual MRP genes expressed in HTM cells was confirmed additionally based on direct sequencing of the respective PCR-derived DNA fragments (Fig. 1A).

The presence of MRP4 protein in HTM cells was also examined by immunoblot analysis using an MRP4-specific polyclonal antibody. MRP4-specific immunoreactivity (a closely migrating doublet of ~150 kDa) was easily detectable in total cell lysate and membrane-enriched fractions, but not in the soluble fraction (40,000*g* supernatant) of HTM cells, as shown in Figure 1B. The doublet protein bands may represent potential posttranslational modification derivatives perhaps via phosphorylation. To examine the distribution profile of MRP4 in the AH outflow pathway, formalin-fixed paraffin-embedded human donor eyes (whole globe sections; donor subjects aged 73 and 92 years) were examined by immunohistochemical fluorescence detection, which revealed MRP4 immunoreactivity throughout the AH outflow pathway including TM, SC, and juxtacanalicular tissue (JCT), with a relatively higher staining intensity in TM tissue relative to the ciliary body (Fig. 1C). As expected, the staining pattern appears to be membrane localized in cells of the outflow pathway. Data derived from a 92-year-old donor specimen are shown in Figure 1C.

Effects of MRP4 Inhibition on TM Cell Morphology and Actin Cytoskeletal Organization

To explore a possible role for the MRP4/5 proteins in regulation of TM cell morphological characteristics, serum-starved (24 hours) HTM cells were treated with either MK571 (10–100 μM), a high affinity MRP4 inhibitor, or with a broad range of inhibitors of MRPs (not specific to any particular MRP) including quercetin (10–100 μM) or probenecid (0.1–1 mM). Time-dependent changes in cell morphology were then followed by viewing cultures using phase contrast microscopy. HTM cells treated with MK571, quercetin or probenecid exhibited dose-dependent changes in cell morphology by 1 hour after addition of inhibitor drugs (data not shown). Figure 2A shows cell shape changes elicited by 90 minute of treatment with 50 μM MK571 and quercetin, and 1 mM probenecid. These drugs induced cell rounding, filamentous, and relaxed morphology mimicking the changes induced in response to Rho kinase inhibitor treatment, as reported earlier (Fig. 2A).[18] These drug-induced morphological changes were rapidly reversed (within 20–30 minutes, data not shown) upon washout of drugs, with TM cells recovering normal morphology. Drug treated TM cells did not exhibit any noticeable cytotoxic responses to the MRP inhibitors used in this study, as assessed by live cell fluorescein diacetate and propidium iodide staining (data not shown).[39]

The morphological changes induced by a 90 minute treatment of HTM cells with MK571 (50 μM), quercetin (50 μM), or probenecid (1 mM) were associated with a dramatic decrease in FITC-phalloidin stained actin stress fibers (Fig. 2B). A significant decrease in MLC phosphorylation, a key regulator of myosin II activity, was also evident in these MRP inhibitor treated TM cells, as assessed by immunoblot analysis of total cell lysates using anti-phospho-MLC antibody (Figs. 2C, 2D). These results were based on a minimum of four independent analyses.

Effects of MRP4 Inhibition on Levels of Intracellular cAMP and cGMP in HTM Cells

To explore whether the above described changes in cell morphology, actin cytoskeleton and phospho-MLC induced by MRP inhibitors were associated with alterations in the levels of cyclic nucleotides, we examined the effects of MK571 on cAMP and cGMP levels in HTM cells using an ELISA. These analyses were performed both, in the presence and absence of the cyclic nucleotide phosphodiesterase inhibitor, IBMX (3-Isobutyl-1-methylxanthine). Treatment of serum starved HTM cells with MK571 (50 μM for 45 minutes) resulted in a significant increase in both cAMP and cGMP levels (6×-fold and 5.1×-fold, respectively; $n = 4$, $P < 0.02$, results presented as nM per 5×10^4 cells, Fig. 3A). Similarly, IBMX treatment (25 μM) for 45 minutes yielded significant increases in both cAMP and cGMP levels (6.5×- and 5.7×-fold, respectively; Fig. 3A). The pretreatment with IBMX (25 μM) for 15 minutes followed by inhibition of MRP4 using MK571 (50 μM) for 30 minutes

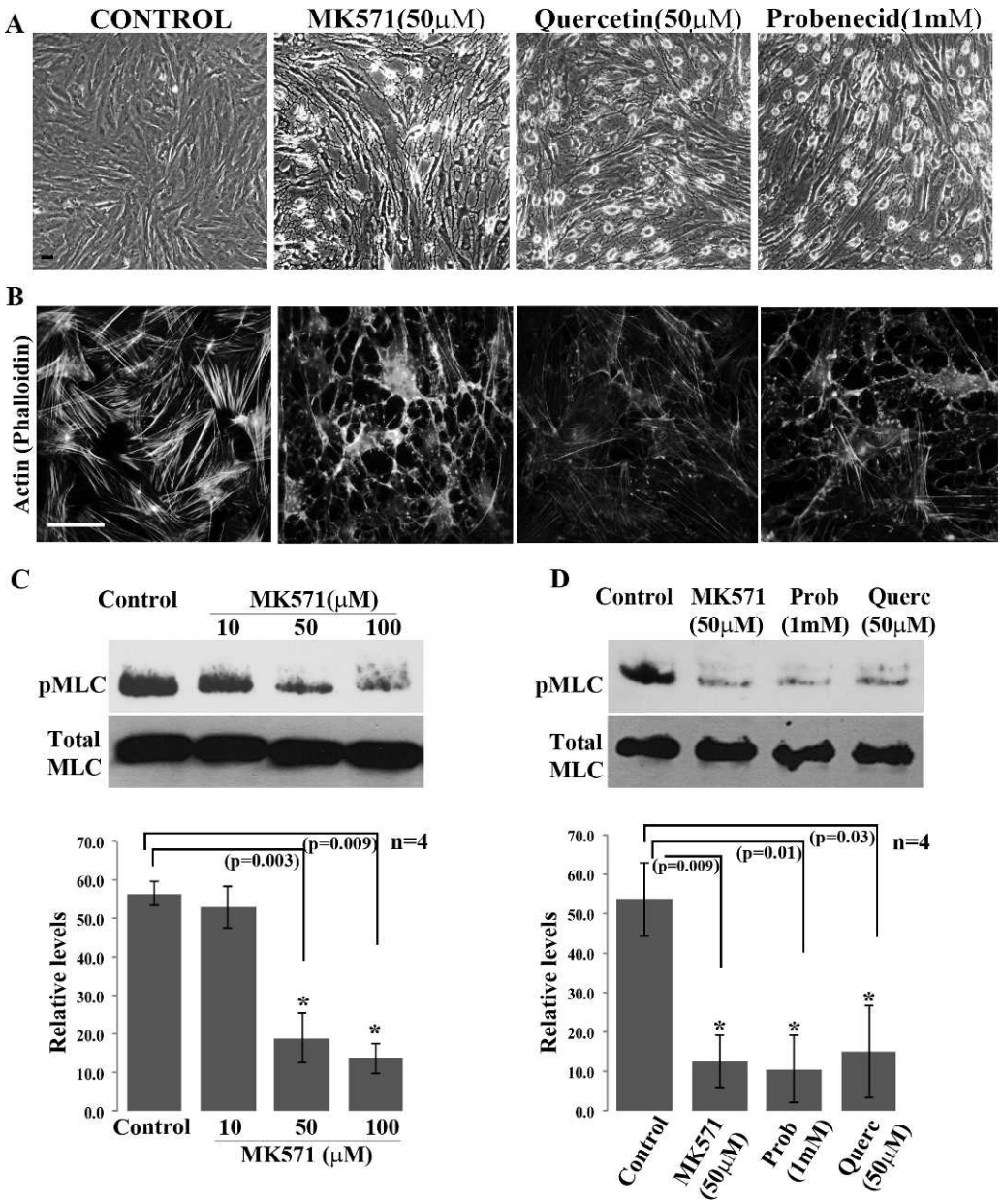

Figure 2. Effects of MRP4 inhibition on HTM cell morphology, actin cytoskeleton and MLC phosphorylation. (**A**) Treatment with MRP inhibitors including MK571 (50 μM), quercetin (50 μM), and probenecid (1 mM) for 90 minutes induced morphological changes in serum-starved (24 hours) HTM cells. Representative phase contrast images show TM cells exhibiting a relaxed and filamentous morphology with cell–cell detachment. (**B**) FITC-phalloidin based F-actin staining shows a dramatic loss of actin stress fibers in the MRP inhibitor treated TM cells described in panel (**A**). Microscope objective: 40×. *Scale bars*: 50 μm. (**C**) Immunoblotting analysis showing a dose-dependent decrease in phospho-MLC in HTM cells treated for 90 minutes with 10, 50, and 100 μM of MK571. The 50 and 100 μM concentrations of MK571 yielded a significant (*$P < 0.01$) decrease in pMLC, as revealed by densitometric quantification (histograms). (**D**) Similar to the effects of MK571 (50 μM), probenecid (1 mM, 90 minutes) and quercetin (50 μM, 90 minutes) treatment also led to significant decreases in phospho-MLC levels in HTM cells. Histograms are based on mean ± SD of four independent experiments (*$P < 0.05$).

resulted in higher increase in the levels of cAMP and cGMP beyond that elicited by either inhibitor alone (7.6×- and 8.7×-fold, respectively (Fig. 3A; $n = 4$).

Based on the foregoing results, we sought to identify the existence of a potential interrelationship between the elevation of cAMP/cGMP levels and cell relaxation characteristics in HTM cells, and also evaluated actin cytoskeletal integrity and MLC phosphorylation in the same experiments. As described earlier (Figs. 2B, 2C), MK571 treatment causes significant reduction in actin stress fibers and phospho-MLC levels in TM cells (Figs. 3B, 3C), following 90 minutes of drug exposure. Similar responses were also triggered by IBMX treatment, which significantly reduced both actin stress fibers and phospho-MLC levels in HTM cells over the same time course (90 minute treatment, Figs. 3B, 3C). The combination of both MK571 and IBMX yielded a maximum reduction in phospho-MLC in TM cells (Fig. 3C). These results were based on four independent analyses.

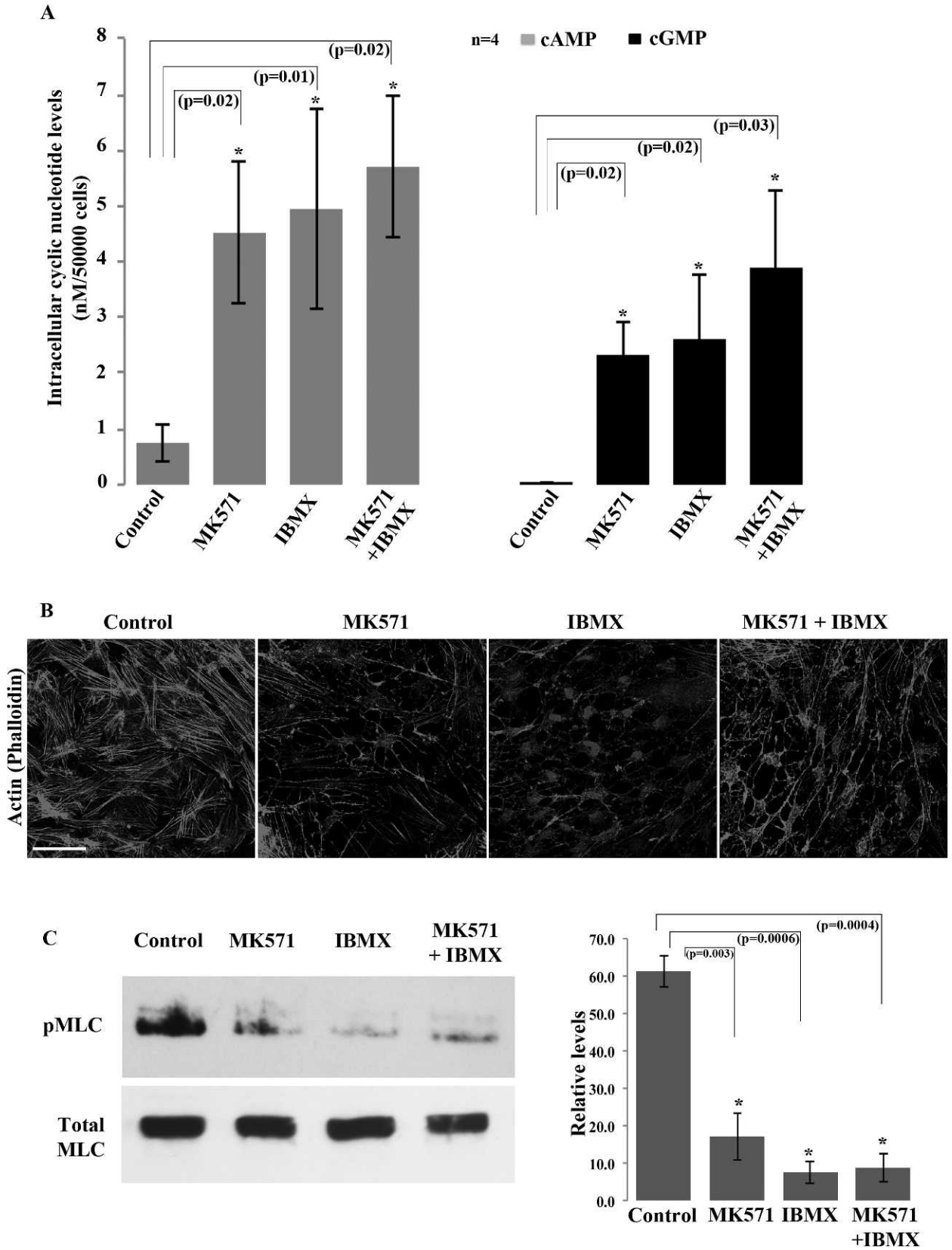

Figure 3. Increased intracellular cAMP and cGMP levels in HTM cells treated with inhibitors of MRP4. Total cellular cAMP and cGMP levels were determined by ELISA as described in the Material and Methods section. (**A**) Serum-starved (24 hours) HTM cells treated with MK571 (50 μM) or IBMX (25 μM; Phosphodiesterases inhibitor) for 45 minutes exhibited significant increases in the intracellular levels of both cAMP and cGMP (>5-fold expressed as nanomolar per 5×10^4 TM cells). Pretreatment with 25 μM IBMX (for 15 minutes) followed by MK571 (50 μM for 30 minutes) led to a synergistic increase in the levels of cAMP and cGMP (7.6- and 8.7-fold, respectively, relative to untreated controls) compared with treatment with either drug alone and untreated controls. Histograms represent the mean ± SD of four independent experiments with triplicate analysis per

sample (*$P < 0.05$). (**B**) Staining for F-actin using FITC-phalloidin shows a dramatic decrease in actin stress fibers in serum-starved HTM cells treated with either MK571 (50 μM) or IBMX (25 μM) for 90 minutes, or in combination (pretreatment with 25 μM IBMX followed by 50 μM MK571 for 75 minutes), relative to untreated control cells. Microscope objective: 40×. *Scale bar*: 50 μm. (**C**) Phospho-MLC levels were decreased significantly in HTM cells (serum-starved for 24 hours) treated with either MK571 (50 μM) or IBMX (25 μM) for 90 minutes each, or in combination as described in this legend. The histogram shows quantitative changes in pMLC levels, as derived from densitometric analysis of four independent experiments (mean ± SD) (*$P < 0.05$).

Effects of siRNA-Based Suppression of MRP4 Expression in HTM Cells

In addition to using the pharmacological approach, we also employed siRNA-based suppression of MRP4 expression to confirm a definitive and specific role for this protein in regulating the morphological and relaxation characteristics of TM cells. HTM cells transfected with MRP4-specific siRNA exhibited a significant decrease (~90% at 82 hours after siRNA treatment; $n = 4$) in MRP4 protein levels relative to cells treated with scrambled control siRNA, based on immunoblotting analysis using total cell lysates (Fig. 4A). HTM cells treated with MRP4 siRNA also exhibited differences in cell morphology relative to those treated with the scrambled control siRNA, exhibiting a filamentous morphology similar to MK571 treated cells (Fig. 4B, see arrows). Additionally, the MRP4 siRNA treated HTM cells also revealed decreased actin stress fiber staining as determined using TRITC-phalloidin (Fig. 4C), as well as a significant decrease in MLC phosphorylation (Fig. 4D; $n = 4$), compared with scrambled siRNA treated control cells.

Effects of MK571 on PKA and PKG Activities in HTM Cells

Since MK571 treated TM cells exhibited decreases in actin stress fibers and MLC phosphorylation, which are considered hallmarks of cellular relaxation, together with changes in cell shape and intracellular levels of cAMP and cGMP, we designed experiments to explore the signaling mechanisms downstream of cAMP and cGMP generation that might account for the relaxation response observed in TM cells. For this, we first examined changes in phosphorylation status of RhoA and MLC phosphatase (MYPT1 subunit) using phospho-specific RhoA serine 188 and MYPT1 Thr 696 antibodies, since these signaling molecules play a critical role in regulation of cellular contractile force.[41] Phosphorylation is known to negatively influence the activity of RhoA and stimulate the activity of MYPT1, thereby leading to cellular relaxation.[21,42–44] HTM cells treated with MK571 (50 μM) or probenecid (1 mM) for 90 minutes exhibited no significant differences in phosphorylation status of either RhoA or MYPT1 relative to untreated control specimens, as assessed by immunoblotting analysis and subsequent densitometric quantification using total cell lysate protein (Fig. 5A; $n = 4$).

We then explored the possible involvement of PKA and PKG signaling in the observed effects of MK571 on HTM cells, as these two enzymes are well recognized to play a key role in relaxation biology upon activation by cAMP and cGMP, respectively.[21,45] Toward this objective, we first examined the effects of preblocking the activity of PKA and PKG in TM cells using Rp-8-Br-2′-O-MB-cAMPS and Rp-8-Br-cGMPS, respectively, followed by treatment with MK571, and assessment of changes in cell morphology, actin stress fiber organization and MLC phosphorylation, relative to TM cells treated with MK571 alone. Pretreatment of HTM cells with the PKA inhibitor (Rp-8-Br-2′-O-MB-cAMPS) did not impact the ability of MK571 to cause changes in cell shape (not shown), or decreases in actin stress fibers (Fig. 5C) and phospho-MLC (Fig. 5B). However, pretreatment of HTM cells with the PKG inhibitor (Rp-8-Br-cGMPS) suppressed the ability of MK571 to mediate changes in cell shape, actin stress fibers (Fig. 5C) and phospho-MLC levels (Fig. 5B), indicating the participation of PKG in MK571-induced changes in the cellular relaxation characteristics of TM cells.

To obtain further confirmation of the participation of either PKA or PKG or both in mediating the effects of MK571 in TM cells, we examined the differential phosphorylation status of VASP by PKA and PKG. VASP is a well characterized member of the Ena-VASP family of proteins involved in actin cytoskeletal organization and cell-ECM interactions.[46] PKA and PKG phosphorylate VASP at Ser 157 and Ser 239, respectively, and regulate VASP activity.[38] Cellular VASP has been used extensively as a test substrate to evaluate PKA and PKG activation in response to alterations in intracellular levels of cyclic nucleotides.[38,47] We used this approach to examine MK571-induced changes in activation of PKA or PKG signaling in HTM cells in the presence and absence of Rp-8-Br-2′-O-MB-cAMPS and Rp-8-Br-cGMPS, as described above. Under these conditions, we found that inhibition of PKA by Rp-8-Br-2′-O-MB-cAMPS alone did not alter VASP Ser 157 phosphorylation significantly (Fig. 6). However, blocking MRP4 with MK571 alone or preblocking PKA followed by MRP4 inhibition led to an increase in VASP Ser 239 phosphorylation by 2.8-fold ($P < 0.022$, $n = 4$) or 2.5-fold ($P < 0.038$, $n = 4$), respectively (Fig. 6). In contrast, preblocking PKG activity with Rp-8-Br-cGMPS, followed by MRP4 inhibition using MK571, abrogated the increase in VASP Ser 239 phosphorylation indicating the preferential activation of PKG by MK571 treatment, and a requirement of PKG activity to regulate cellular relaxation via the nucleotide efflux channel activity of MRP4 (Fig. 6). As known for other cell types,[38] immunoblotting analysis of HTM cell pVASP Ser 239 exhibited a doublet comprised of two closely migrating bands, the upper band of which was used for monitoring densitometry-based quantitative changes as shown in Figure 6.

Effects of Topical Administration of MK571 on IOP of Dutch-Belted Rabbits

Four Dutch-Belted male rabbits were used for this experiment. Prior to drug (MK571) treatment, baseline values of IOP were measured in both the right and left eyes at least twice with a 48 hour interval between measurements. Two concentrations (0.1 and 0.2%; representing 18.6 and 37.2 mM, respectively) of MK571 dissolved in PBS were used. The 0.2% concentration of drug was the maximum dose that was found to be suitable based on solubility in PBS. Topical application (one time) of 0.2% MK571 solution induced a significant decrease (~18%, $P < 0.03$; $n = 8$) in IOP within 1 hour of drug application (Fig. 7). The drug effect was consistent in all four rabbits tested. IOP was found to return to baseline values by 2 hours following drug administration and to stay at basal level for the next 24 hours (Fig. 7). The IOP lowering effect of MK571 (0.2%) was consistent over two independent experiments conducted using the same rabbits and two different doses of drug. Between the two tests and two doses, we ensured a minimum gap of one week and also confirmed that the rabbits had attained normal IOP prior to starting each drug test. Figure 7

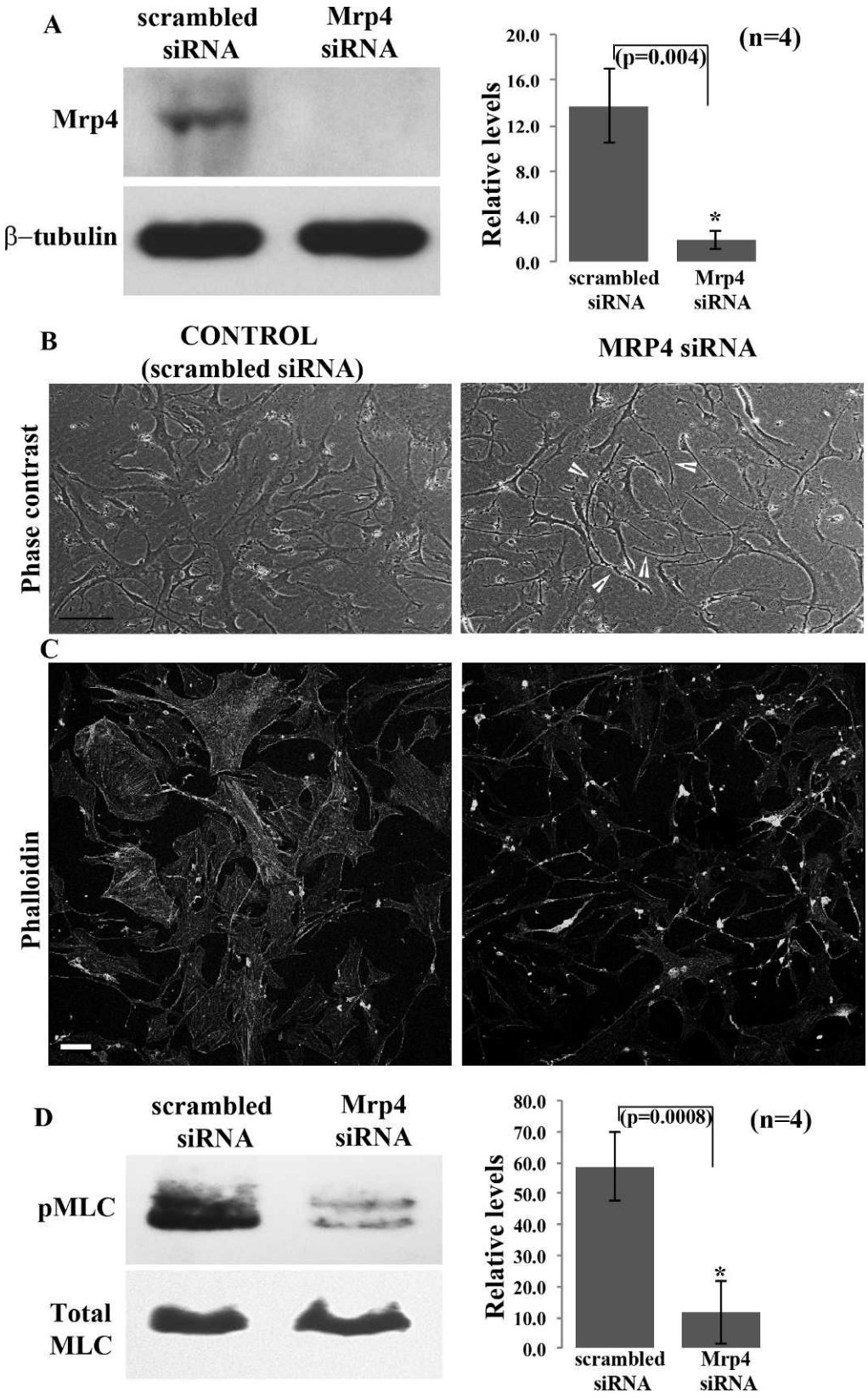

Figure 4. Effects of siRNA-mediated knockdown of MRP4 expression on HTM cell morphology, actin cytoskeleton and phospho-MLC. (**A**) Primary HTM cell cultures transfected with human MRP4 specific siRNA for 80 hours showed a significant knockdown (>80%) of MRP4 protein levels relative to cells transfected with a scrambled siRNA control, based on immunoblotting analysis. β-tubulin was probed as a loading control. The histogram shows a densitometry-based representation of the decrease in MRP4 protein levels (values are mean ± SD, $n = 4$, $^*P < 0.05$). (**B**) Phase contrast images depict altered cell morphology and (**C**) decreased actin stress fibers in MRP4 siRNA treated HTM cells relative to cells treated with the scrambled siRNA control. Microscope objective: 40×. *Scale bar*: 50 μm. (**D**) The decreased MRP4 levels in the MRP4-siRNA transfected HTM

cells was associated with a significant decrease in phospho-MLC levels compared with cells treated with the scrambled siRNA controls. The histogram shows densitometry-based differences in protein levels of phospho-MLC as derived from four independent experiments. Total MLC was immunoblotted in the same samples as a loading control (*$P < 0.05$).

shows the data derived from the mean values of eight independent observations (pooled data from the first and second tests performed on four different rabbits each time). As shown in Figure 7, the 0.1% dose of MK571 did not cause significant differences in IOP relative to sham treated controls ($n = 8$). During the topical drug tests in rabbits, we also monitored ocular changes including tearing, eye lid swelling, ocular hyperemia, and irritation. There was no notable change in any of these aspects other than the IOP-lowering response upon drug application.

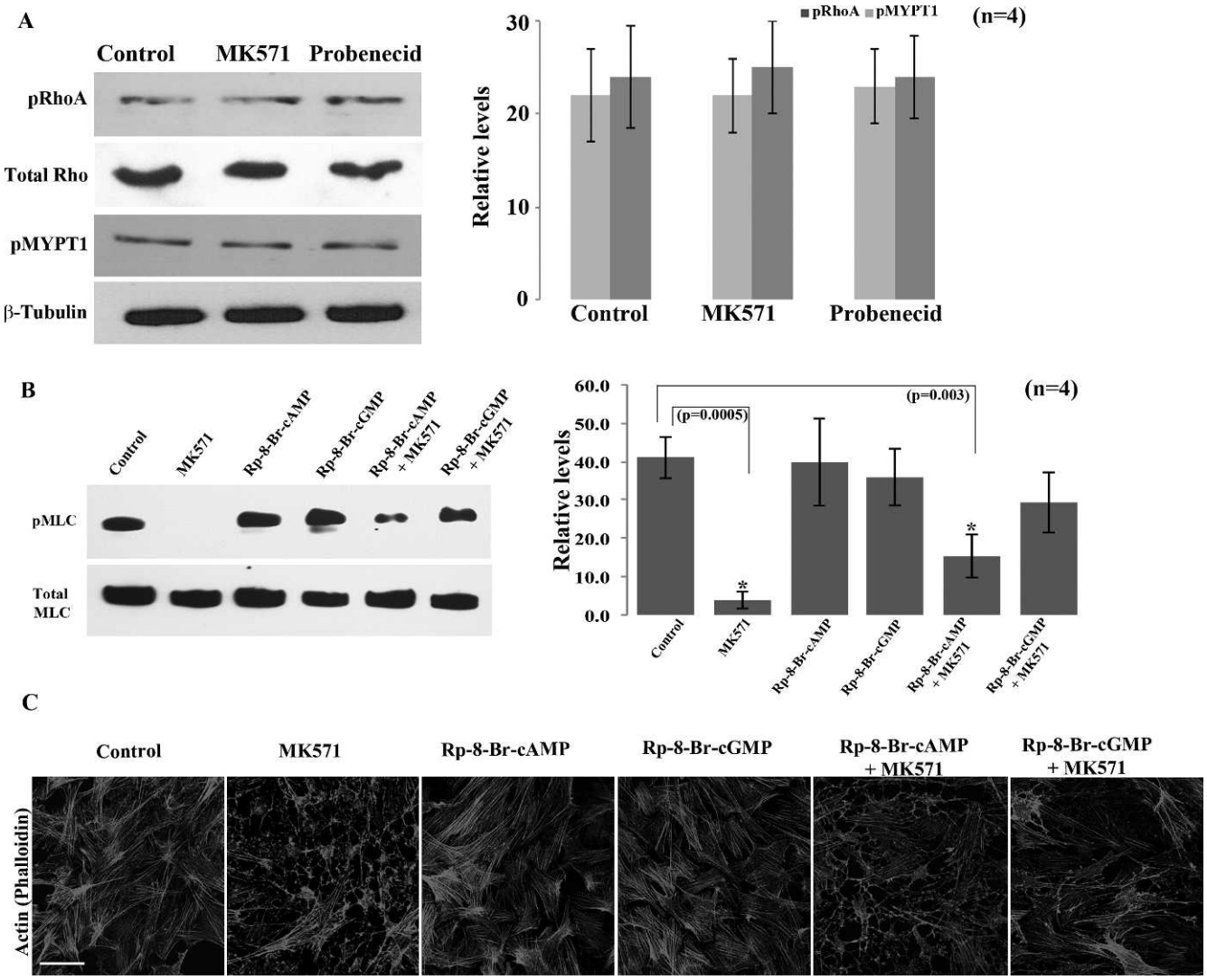

Figure 5. Preferential activation of PKG-mediated cellular relaxation in HTM cells treated with MK571. (**A**) Serum-starved (24 hours) confluent cultures of HTM cells treated with either MK571 (50 μM) or probenecid (1 mM) showed no changes in the phosphorylation status of RhoA Ser 188 and myosin phosphatase target subunit 1 (MYPT1 Ser 696) and levels of total RhoA, relative to untreated controls. Total RhoA and β-tubulin were probed as loading controls. Histograms show the densitometry-based relative levels (mean ± SD; $n = 4$) of the different proteins of interest. (**B**, **C**) To explore whether PKA and PKG mediated events downstream of the MK571-stimulated increase in cAMP and cGMP in HTM cells play a role in the regulation of MLC phosphorylation (**B**) and actin cytoskeletal organization (**C**) was assessed. Serum-starved HTM cells were treated with either MK571 (50 μM), PKA inhibitor, Rp-8-Br-2′-O-MB-cAMPS (50 μM) or PKG inhibitor, Rp-8-Br-cGMPS (50 μM) alone for 90 minutes, or pretreated with these selective kinase inhibitors for 30 minutes followed by MK571 for 90 minutes, and then examined for changes in pMLC and actin stress fibers by immunoblotting and FITC-phalloidin staining, respectively. Treatment of HTM cells with PKA and PKG inhibitors alone did not cause any significant changes in the levels of pMLC as compared with a dramatic decrease (*$P < 0.005$) in the MK571 treated cells. However, while there was no significant difference in the levels of pMLC in cells pretreated with PKG inhibitor (Rp-8-Br-cGMPS) followed with MK571 treatment, there was a significant decrease in the TM cells pretreated with PKA inhibitor (Rp-8-Br-2′-O-MB-cAMPS) (*$P < 0.003$). Under similar conditions, consistent to changes noted in pMLC, F-actin staining by TRITC-phalloidin revealed no effect by the PKG or PKA inhibitors relative to a dramatic decrease in the MK571 treated cells. However, while there was a decrease in F-actin staining in PKA inhibitor and MK571 treated cells, there was no difference in the cells treated with PKG inhibitor and MK571. Microscope objective: 40×, *Scale bar*: 50 μm. These observations collectively reveal the preferential activation and involvement of cGMP-dependent PKG signaling in response to elevation in cyclic nucleotides driven by MRP4 inhibition in HTM cells.

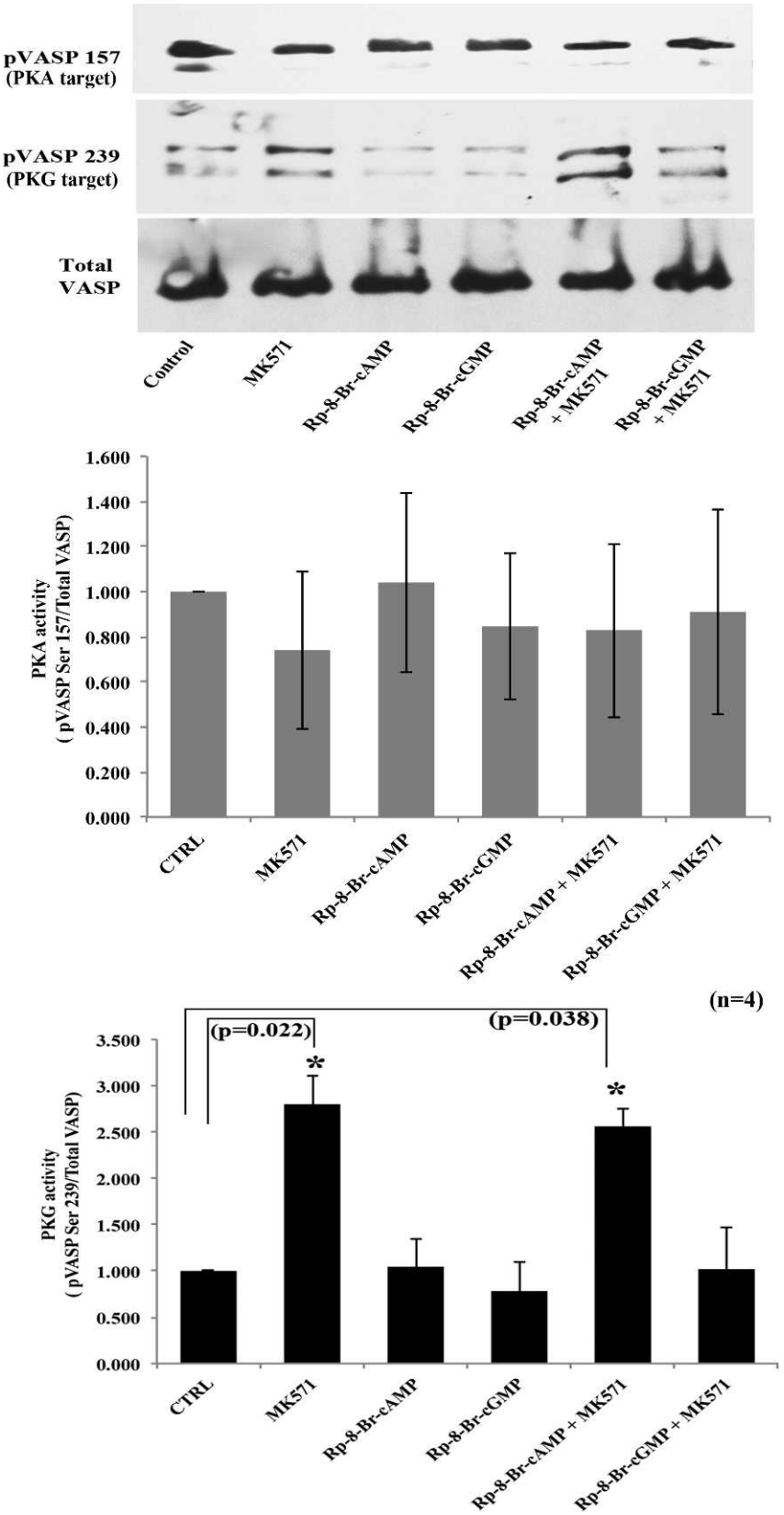

Figure 6. Preferential activation of PKG-mediated cellular relaxation in HTM cells treated with MK571. Differential phosphorylation of VASP was analyzed to explore PKA and PKG activation in MK571 treated TM cells. These experiments probed for VASP phosphorylation at Ser 157 and Ser 239 by immunoblotting analysis using the respective phospho-specific antibodies, in HTM cells treated with PKA and PKG specific inhibitors and control cells as described in Figure 5B. Treatment of HTM cells with MK571 alone or in the presence of either PKA or PKG inhibitors did not have any effect on the phosphorylation of pVASP Ser 157 indicating that PKA did not play a significant role in the MK571-mediated events in these cells. On the other hand, under similar conditions, MK571 treatment led to an increase in VASP Ser 239 phosphorylation, which was not blocked in cells

treated with MK571 and PKA inhibitor, but was suppressed in cells treated with both, MK571 and the PKG inhibitor, indicating a preferential activation of PKG in MK571 treated HTM cells. Phospho-VASP was normalized to total VASP protein levels based on immunoblotting analysis. Total VASP levels were found to be unaltered in the experiments described above. Values represent mean ± SD of four independent experiments (*$P <$ 0.05).

Discussion

While the contractile and relaxation characteristics of TM tissue have long been recognized to influence AH outflow facility and homeostasis of IOP, the molecular mechanisms underlying regulation of these cellular responses are not well understood.[7] In this study we examined for the first time the expression and distribution profile of MRP4, a cyclic nucleotide efflux regulating multidrug-resistance–associated transport protein in TM cells and determined its potential role in modulation of IOP in a rabbit model. This study reports on the distribution profile of MRP4 in the human AH outflow pathway, and demonstrates that pharmacologic inhibition of MRP4 induces TM cellular relaxation as reflected by decreases in MLC phosphorylation and actin stress fibers, and an elevation in intracellular levels of cAMP and cGMP in the cultured TM cells. Importantly, topical application of MRP4 inhibitor (MK571) was found to significantly lower IOP in rabbits. Mechanistically, the MK571-induced decrease in MLC phosphorylation and ensuing cellular relaxation in TM cells appears to be mediated predominantly via the cGMP-activated PKG pathway (Fig. 8). Taken together, these observations suggest that the cAMP and cGMP efflux regulating ABCC transporters (e.g., MRP4 and MRP5) play a significant role in homeostasis of IOP by controlling potentially the relaxation characteristics of tissues in the AH outflow pathway.

Various cellular mechanisms regulating the relaxation characteristics of AH outflow pathway including nitric oxide, adenylate cyclase, guanylate cyclase, cAMP, cGMP, and cyclic nucleotide-dependent phosphodiesterases have been documented to increase AH outflow and lower IOP in different model systems, indicating the importance of cyclic nucleotides and their metabolizing enzymes in homeostasis of IOP.[7,19,20,30,48–55] However, while the synthesis and degradation of cAMP and cGMP, which activate PKA and PKG, respectively, and regulate relaxation characteristics of smooth muscle and nonmuscle tissues are regulated predominantly by adenylate and guanylate cyclases and phosphodiesterases, the intracellular levels of cyclic nucleotides are also controlled by membrane transporter-mediated cellular efflux.[31] MRP4 and MRP5, which belong to the ABCC subfamily of multidrug-associated resistance proteins, are recognized to pump various organic anionic compounds out of cells.[31] Importantly, in addition to various drugs and drug metabolites, MRP4 and MRP5 mediate efflux of endogenous organic compounds, especially cyclic nucleotides, in an energy-dependent manner, thereby influencing different cellular responses.[31,38] Since MRP4/5 are known to influence the relaxation properties of various cell types by regulating intracellular levels of cAMP and cGMP,[38,56] we were interested in determining the role of MRP4 in TM cell relaxation and homeostasis of IOP.

As determined by immunoblotting and immunofluorescence analyses both cultured human TM cells and AH outflow

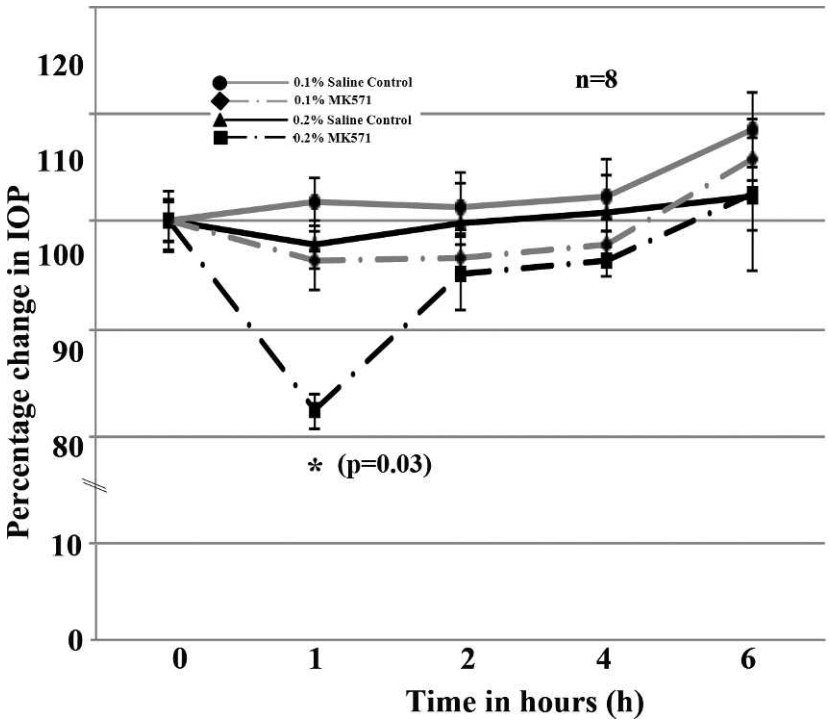

Figure 7. Effects of topical administration of MK571 on IOP of rabbits. MK571 was topically applied at two different dosages (0.1% or 0.2% dissolved in PBS) to Dutch-belted male rabbit eyes, and changes in IOP determined using a pneumotonometer. IOP measurements were acquired in a time dependent manner starting from 1 hour after drug application. The 0.2% (37.2 mM) dose of MK571 caused a significant decrease in IOP (~18% compared with sham control [PBS] eyes, *$P <$ 0.03). The IOP-lowering effect of MK571 was found to be significant at 1 hour post drug application, and rebounds to close to basal or normal levels by the second hour following drug administration, and remains at basal values thereafter. Statistical significance was determined based on Wilcoxon rank-sum test (*$P <$ 0.03).

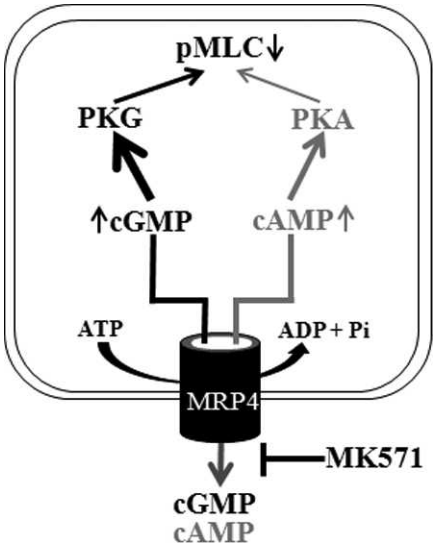

Figure 8. The schematics of MRP4 regulated efflux of cAMP and cGMP and its inhibition by MK571 leads to increased levels of intracellular cAMP and cGMP and activation of PKA and PKG. *Bold arrows* indicate a preferential activation of PKG in HTM cells treated with MK571under the conditions described in this study.

pathway tissues including the TM, SC, and the JCT region expressed MRP4. Importantly, inhibition of MRP4 in cultured HTM cells using both selective (MK571) and nonselective inhibitors (probenecid and quercetin) of MRP4 confirmed a significant role for this transport protein in maintaining cell morphology and actin cytoskeletal organization. Significantly, drug treatment evoked the appearance of cellular relaxation morphology in TM cells, together with a reduction in actin stress fibers and a marked decrease in phosphorylation of MLC, which is a key regulator of myosin II that controls the cell contractile and relaxation characteristics via its interaction with actin filament.[41] A noteworthy observation is that the MK571-induced morphological changes in TM cells were found to be rapidly (in less than 20 minutes) reversible upon removal of drug from cell culture media, indicative of a fast rate of cyclic nucleotide efflux via MRP4. Importantly, the decrease in actin stress fibers and phospho-MLC in MK571-treated HTM cells was associated with a robust increase (by >5-fold) in the levels of both cAMP and cGMP in TM cells. This increase in intracellular levels of cyclic nucleotides was further heightened in the presence of IBMX, a well characterized inhibitor of phosphodiesterases, demonstrating the significance of both phosphodiesterases and MRP4 in maintaining intracellular cyclic nucleotides in TM cells. Although MK571 is known to also inhibit MRP1, inhibition or downregulation of MRP1 does not result in changes in the intracellular levels of cyclic nucleotides.[38,57] Similarly, probenecid and quercetin also inhibit other MRP transporters, but only MRP4 and MRP5 have been demonstrated to regulate the efflux of cyclic nucleotides and relaxation signaling.[38,57] Furthermore, the pharmacologic effects of MK571 in TM cells were found to be consistent with those caused by MRP4 deficiency achieved by the use of siRNA methodology, confirming a specific role for MRP4 in regulating cellular relaxation and homeostasis of intracellular cyclic nucleotides.

To seek mechanistic insight into how the elevated levels of cyclic nucleotides may lead to MK571-induced cellular relaxation in TM cells, we probed whether PKA and PKG, whose activity is known to be directly regulated by cAMP and cGMP, respectively,[21,58] might participate in mediating the effects of MK571. Experiments performed using specific inhibitors of PKA (Rp-8-Br-2′-O-MB-cAMPS) and PKG (Rp-8-Br-cGMPS) and a well characterized endogenous substrate of these enzymes, VASP,[38] confirmed activation of PKG in TM cells treated with MK571. For example, phosphorylation of VASP Ser 239, which is regulated by PKG, was decreased significantly in TM cells pretreated with PKG inhibitor (Rp-8-Br-cGMPS), but not the PKA inhibitor (Rp-8-Br-2′-O-MB-cAMPS) prior to MK571 exposure, confirming preferential activation of PKG relative to PKA under the conditions described in this study. In contrast, phosphorylation of VASP Ser 157, which is known to be regulated specifically by PKA, was found to be unaltered in TM cells treated with MK571. To obtain further confirmation for the preferential activation of PKG in MK571 treated TM cells, we evaluated changes in phospho-MLC levels in these cells. The MK571-mediated decrease in MLC phosphorylation in TM cells was inhibited significantly in the presence of PKG inhibitor (Rp-8-Br-cGMPS), but not by the PKA inhibitor (Rp-8-Br-2′-O-MB-cAMPS).

Although PKA has been reported to phosphorylate RhoA at Ser 188 leading to its inactivation in different cell types including TM cells,[42,59] MK571-treated TM cells exhibited neither changes in RhoA Ser188 phosphorylation nor inactivation of the RhoA/Rho kinase signaling pathway, which can lead to cellular relaxation via downregulating MLC phosphorylation as we reported earlier.[18] Myosin phosphatase plays an important role in cellular relaxation by downregulating MLC phosphorylation. Rho kinase is known to phosphorylate and inactivate myosin phosphatase in a calcium-independent manner, leading to increased MLC phosphorylation.[41,44] Analysis of the phosphorylation status of myosin phosphatase showed no changes in MK571-treated TM cells, indicating that the Rho A/Rho kinase pathway does not play a significant role in MK571-induced cellular relaxation in HTM cells under the conditions described in this study.

Although our studies on the effects of MK571 in TM cells indicate activation of PKG, it is not clear how this activation leads to cellular relaxation and decreases MLC phosphorylation and actin stress fibers. Since we obtained experimental evidence to rule out a significant role for the RhoA/Rho kinase pathway in MK571-induced cellular relaxation, it is reasonable to speculate the effects of MK571 could be related to calcium/calmodulin-dependent MLC kinase, whose activity is closely dependent on calcium channel protein activity.[21,41] Both PKG and PKA are known to regulate calcium influx and efflux through their direct and indirect role in regulating the activity of various calcium channel proteins.[21,60,61] Therefore, it is possible that the MK571-induced increase in intracellular cyclic nucleotide levels along with PKG and PKA in TM cells may influence calcium homeostasis by acting directly on the channel proteins leading to cellular relaxation. Additionally, elevated levels of cyclic nucleotides in TM cells may likely have effects on TM cell volume, which is relevant to AH outflow as reported earlier.[30]

Finally, in experiments to determine whether the effects of MK571-induced cellular relaxation of TM cells translates into physiologic correlates at the level of IOP in the in vivo setting, topical application of MK571 in Dutch-belted rabbits led to a significant decrease in IOP. This response was consistent with the known response of IOP to various agents that elevate cAMP and cGMP, including nitric oxide, adenosine, and inhibitors of phosphodiesterases, as well as the direct effects of these nucleotides on IOP.[7,19,25,30,48,50–55] Under our experimental conditions, the ocular hypotensive response of MK571 (0.2%) was transient, the effect lasting for less than 2 hours. Although the reasons for the transient nature of this response are not clear, several possibilities could account for the observation, including shorter bioavailability and stability of MK571, and

limited corneal penetration of drug. Interestingly, unlike prostaglandins and Rho kinase inhibitors,[5,17,62] topical application of 0.2% MK571 did not cause noticeable conjunctival redness or hemorrhage. Importantly, the IOP-lowering response of MK571 offers additional insight into the possible utility of a combination of MRP4/5 inhibitors and NO donors, adenosine, or inhibitors of phosphodiesterases, to elicit a maximum IOP lowering response. A systematic evaluation of additional MRP4 inhibitors for IOP-lowering capacity is, therefore, predicted to be of value in this regard. Additionally, MRP4 has been characterized as a highly polymorphic gene.[63] Therefore, it may be interesting to examine its possible association with glaucoma in genetic studies.

Acknowledgments

The authors thank Frans G.M. Russel, Professor of Pharmacology and Toxicology, University of Nijmegen, The Netherlands, for his help in providing human MRP4 antibody, and Alan Proia for human eye whole globe paraffin embedded tissue sections. They also thank Corey Morris for his help with IOP monitoring in rabbits.

References

1. Quigley HA, Broman AT. The number of people with glaucoma worldwide in 2010 and 2020. *Br J Ophthalmol*. 2006;90:262–267.
2. Weinreb RN, Khaw PT. Primary open-angle glaucoma. *Lancet*. 2004;363:1711–1720.
3. Kwon YH, Fingert JH, Kuehn MH, Alward WL. Primary open-angle glaucoma. *N Engl J Med*. 2009;360:1113–1124.
4. Gabelt BT, Kaufman PL. Changes in aqueous humor dynamics with age and glaucoma. *Prog Retin Eye Res*. 2005;24:612–637.
5. Rao VPED. Rho GTPase/Rho kinase inhibition as a novel target for the treatment of glaucoma. *BioDrugs*. 2007;21:167–177.
6. Russell P, Johnson M. Elastic modulus determination of normal and glaucomatous human trabecular meshwork. *Invest Ophthalmol Vis Sci*. 2012;53:117.
7. Wiederholt M, Thieme H, Stumpff F. The regulation of trabecular meshwork and ciliary muscle contractility. *Prog Retin Eye Res*. 2000;19:271–295.
8. Tan JC, Peters DM, Kaufman PL. Recent developments in understanding the pathophysiology of elevated intraocular pressure. *Curr Opin Ophthalmol*. 2006;17:168–174.
9. Pattabiraman PP, Rao PV. Mechanistic basis of Rho GTPase-induced extracellular matrix synthesis in trabecular meshwork cells. *Am J Physiol Cell Physiol*. 2010;298:C749–C763.
10. Epstein DL, Rowlette LL, Roberts BC. Acto-myosin drug effects and aqueous outflow function. *Invest Ophthalmol Vis Sci*. 1999;40:74–81.
11. Tian B, Brumback LC, Kaufman PL. ML-7, chelerythrine and phorbol ester increase outflow facility in the monkey Eye. *Exp Eye Res*. 2000;71:551–566.
12. Khurana RN, Deng PF, Epstein DL, Vasantha Rao P. The role of protein kinase C in modulation of aqueous humor outflow facility. *Exp Eye Res*. 2003;76:39–47.
13. Alexander JP, Acott TS. Involvement of the Erk-MAP kinase pathway in TNFalpha regulation of trabecular matrix metalloproteinases and TIMPs. *Invest Ophthalmol Vis Sci*. 2003;44:164–169.
14. Husain S, Shearer TW, Crosson CE. Mechanisms linking adenosine A1 receptors and extracellular signal-regulated kinase 1/2 activation in human trabecular meshwork cells. *J Pharmacol Exp Ther*. 2007;320:258–265.
15. Wang WH, McNatt LG, Pang IH, et al. Increased expression of the WNT antagonist sFRP-1 in glaucoma elevates intraocular pressure. *J Clin Invest*. 2008;118:1056–1064.
16. Mao W, Millar JC, Wang WH, et al. Existence of the canonical Wnt signaling pathway in the human trabecular meshwork. *Invest Ophthalmol Vis Sci*. 2012;53:7043–7051.
17. Honjo M, Tanihara H, Inatani M, et al. Effects of rho-associated protein kinase inhibitor Y-27632 on intraocular pressure and outflow facility. *Invest Ophthalmol Vis Sci*. 2001;42:137–144.
18. Rao PV, Deng PF, Kumar J, Epstein DL. Modulation of aqueous humor outflow facility by the Rho kinase-specific inhibitor Y-27632. *Invest Ophthalmol Vis Sci*. 2001;42:1029–1037.
19. Gilabert R, Gasull X, Pales J, Belmonte C, Bergamini MV, Gual A. Facility changes mediated by cAMP in the bovine anterior segment in vitro. *Vision Res*. 1997;37:9–15.
20. Bartels SP, Lee SR, Neufeld AH. Forskolin stimulates cyclic AMP synthesis, lowers intraocular pressure and increases outflow facility in rabbits. *Curr Eye Res*. 1982;2:673–681.
21. Murthy KS. Signaling for contraction and relaxation in smooth muscle of the gut. *Annu Rev Physiol*. 2006;68:345–374.
22. Derbyshire ER, Marletta MA. Structure and regulation of soluble guanylate cyclase. *Annu Rev Biochem*. 2012;81:533–559.
23. Moncada S, Palmer RM, Higgs EA. Nitric oxide: physiology, pathophysiology, and pharmacology. *Pharmacol Rev*. 1991;43:109–142.
24. Zhou L, Thompson WJ, Potter DE. Functional identification of phosphodiesterase activity in human trabecular meshwork cells. *J Ocul Pharmacol Ther*. 2000;16:317–322.
25. Suzuki R, Karageuzian LN, Crean EV, Anderson PJ. Effects of adrenergic agents and phosphodiesterase inhibitors on outflow facility and cell shape of bovine trabecular meshwork. *Jpn J Ophthalmol*. 1997;41:31–37.
26. Zhou L, Thompson WJ, Potter DE. Multiple cyclic nucleotide phosphodiesterases in human trabecular meshwork cells. *Invest Ophthalmol Vis Sci*. 1999;40:1745–1752.
27. Busch MJ, Kobayashi K, Hoyng PF, Mittag TW. Adenylyl cyclase in human and bovine trabecular meshwork. *Invest Ophthalmol Vis Sci*. 1993;34:3028–3034.
28. Zhang X, Wang N, Schroeder A, Erickson KA. Expression of adenylate cyclase subtypes II and IV in the human outflow pathway. *Invest Ophthalmol Vis Sci*. 2000;41:998–1005.
29. Haque MS, Pang IH, Magnino PE, DeSantis L. Activation of phospholipase C and guanylyl cyclase by endothelins in human trabecular meshwork cells. *Curr Eye Res*. 1998;17:1110–1117.
30. Ellis DZ. Guanylate cyclase activators, cell volume changes and IOP reduction. *Cell Physiol Biochem*. 2011;28:1145–1154.
31. Russel FG, Koenderink JB, Masereeuw R. Multidrug resistance protein 4 (MRP4/ABCC4): a versatile efflux transporter for drugs and signalling molecules. *Trends Pharmacol Sci*. 2008;29:200–207.
32. Borst P, Elferink RO. Mammalian ABC transporters in health and disease. *Annu Rev Biochem*. 2002;71:537–592.
33. Schuetz JD, Connelly MC, Sun D, et al. MRP4: a previously unidentified factor in resistance to nucleoside-based antiviral drugs. *Nat Med*. 1999;5:1048–1051.
34. Reid G, Wielinga P, Zelcer N, et al. The human multidrug resistance protein MRP4 functions as a prostaglandin efflux transporter and is inhibited by nonsteroidal antiinflammatory drugs. *Proc Natl Acad Sci U S A*. 2003;100:9244–9249.
35. van Aubel RA, Smeets PH, Peters JG, Bindels RJ, Russel FG. The MRP4/ABCC4 gene encodes a novel apical organic anion transporter in human kidney proximal tubules: putative efflux pump for urinary cAMP and cGMP. *J Am Soc Nephrol*. 2002;13:595–603.
36. Wielinga PR, van der Heijden I, Reid G, Beijnen JH, Wijnholds J, Borst P. Characterization of the MRP4- and MRP5-mediated

transport of cyclic nucleotides from intact cells. *J Biol Chem*. 2003;278:17664–17671.

37. Sassi Y, Lipskaia L, Vandecasteele G, et al. Multidrug resistance-associated protein 4 regulates cAMP-dependent signaling pathways and controls human and rat SMC proliferation. *J Clin Invest*. 2008;118:2747–2757.
38. Hara Y, Sassi Y, Guibert C, et al. Inhibition of MRP4 prevents and reverses pulmonary hypertension in mice. *J Clin Invest*. 2011;121:2888–2897.
39. Pattabiraman PP, Lih FB, Tomer KB, Rao PV. The role of calcium-independent phospholipase A2gamma in modulation of aqueous humor drainage and Ca2+ sensitization of trabecular meshwork contraction. *Am J Physiol Cell Physiol*. 2012;302:C979–C991.
40. Iyer P, Lalane R III, Morris C, Challa P, Vann R, Rao PV. Autotaxin-lysophosphatidic acid axis is a novel molecular target for lowering intraocular pressure. *PLoS One*. 2012;7: e42627.
41. Fukata Y, Amano M, Kaibuchi K. Rho-Rho-kinase pathway in smooth muscle contraction and cytoskeletal reorganization of non-muscle cells. *Trends Pharmacol Sci*. 2001;22:32–39.
42. Lang P, Gesbert F, Delespine-Carmagnat M, Stancou R, Pouchelet M, Bertoglio J. Protein kinase A phosphorylation of RhoA mediates the morphological and functional effects of cyclic AMP in cytotoxic lymphocytes. *EMBO J*. 1996;15:510–519.
43. Ellerbroek SM, Wennerberg K, Burridge K. Serine phosphorylation negatively regulates RhoA in vivo. *J Biol Chem*. 2003; 278:19023–19031.
44. Feng J, Ito M, Ichikawa K, et al. Inhibitory phosphorylation site for Rho-associated kinase on smooth muscle myosin phosphatase. *J Biol Chem*. 1999;274:37385–37390.
45. Francis SH, Corbin JD. Structure and function of cyclic nucleotide-dependent protein kinases. *Annu Rev Physiol*. 1994;56:237–272.
46. Kwiatkowski AV, Gertler FB, Loureiro JJ. Function and regulation of Ena/VASP proteins. *Trends Cell Biol*. 2003;13: 386–392.
47. Joshi CN, Martin DN, Fox JC, Mendelev NN, Brown TA, Tulis DA. The soluble guanylate cyclase stimulator BAY 41-2272 inhibits vascular smooth muscle growth through the cAMP-dependent protein kinase and cGMP-dependent protein kinase pathways. *J Pharmacol Exp Ther*. 2011;339:394–402.
48. Busch MJ, van Oosterhout EJ, Hoyng PF. Effects of cyclic nucleotide analogs on intraocular pressure and trauma-induced inflammation in the rabbit eye. *Curr Eye Res*. 1992; 11:5–13.
49. Dismuke WM, Mbadugha CC, Ellis DZ. NO-induced regulation of human trabecular meshwork cell volume and aqueous humor outflow facility involve the BKCa ion channel. *Am J Physiol Cell Physiol*. 2008;294:C1378–C1386.
50. Kaufman PL. Adenosine 3′,5′-cyclic-monophosphate and outflow facility in monkey eyes with intact and retrodisplaced ciliary muscle. *Exp Eye Res*. 1987;44:415–423.
51. Kee C, Kaufman PL, Gabelt BT. Effect of 8-Br cGMP on aqueous humor dynamics in monkeys. *Invest Ophthalmol Vis Sci*. 1994;35:2769–2773.
52. Busch MJ, Hoyng PF. Evaluation of IBMX-enhanced ocular hypotension after adrenergic agonists in the rabbit eye. *Graefes Arch Clin Exp Ophthalmol*. 1995;233:296–301.
53. Crosson CE, Gray T. Modulation of intraocular pressure by adenosine agonists. *J Ocul Pharmacol*. 1994;10:379–383.
54. Schneemann A, Dijkstra BG, van den Berg TJ, Kamphuis W, Hoyng PF. Nitric oxide/guanylate cyclase pathways and flow in anterior segment perfusion. *Graefes Arch Clin Exp Ophthalmol*. 2002;240:936–941.
55. Stein PJ, Clack JW. Topical application of a cyclic GMP analog lowers IOP in normal and ocular hypertensive rabbits. *Invest Ophthalmol Vis Sci*. 1994;35:2765–2768.
56. Sassi Y, Abi-Gerges A, Fauconnier J, et al. Regulation of cAMP homeostasis by the efflux protein MRP4 in cardiac myocytes. *FASEB J*. 2012;26:1009–1017.
57. Reid G, Wielinga P, Zelcer N, et al. Characterization of the transport of nucleoside analog drugs by the human multidrug resistance proteins MRP4 and MRP5. *Mol Pharmacol*. 2003; 63:1094–1103.
58. Hofmann F, Feil R, Kleppisch T, Schlossmann J. Function of cGMP-dependent protein kinases as revealed by gene deletion. *Physiol Rev*. 2006;86:1–23.
59. Ramachandran C, Patil RV, Sharif NA, Srinivas SP. Effect of elevated intracellular cAMP levels on actomyosin contraction in bovine trabecular meshwork cells. *Invest Ophthalmol Vis Sci*. 2011;52:1474–1485.
60. Francis SH, Busch JL, Corbin JD, Sibley D. cGMP-dependent protein kinases and cGMP phosphodiesterases in nitric oxide and cGMP action. *Pharmacol Rev*. 2010;62:525–563.
61. Dai S, Hall DD, Hell JW. Supramolecular assemblies and localized regulation of voltage-gated ion channels. *Physiol Rev*. 2009;89:411–452.
62. Williams RD, Novack GD, van Haarlem T, Kopczynski C. Ocular hypotensive effect of the Rho kinase inhibitor AR-12286 in patients with glaucoma and ocular hypertension. *Am J Ophthalmol*. 2011;152:834–841.e1.
63. Abla N, Chinn LW, Nakamura T, et al. The human multidrug resistance protein 4 (MRP4, ABCC4): functional analysis of a highly polymorphic gene. *J Pharmacol Exp Ther*. 2008;325: 859–868.